II.B.2. FaCT: First adaptive CT system

The Center for Gamma-Ray imaging has designed and built an adaptive helical-scan cone beam x-ray micro-CT system to augment its FastSPECT II system and explore adaptive imaging techniques in x-ray computed tomography. Briefly, the system can adjust its magnification and field of view on-the-fly to best suit the object being imaged. These innovations allow us to fit the resolution of the system to the study being performed, and also reduce the overall radiation dose used in a study.

1) Demonstration of non-standard acquisition protocols

We have been able to demonstrate that the non-standard acquisition protocols useful in adaptive x-ray CT are not an impediment to obtaining reconstructed data.

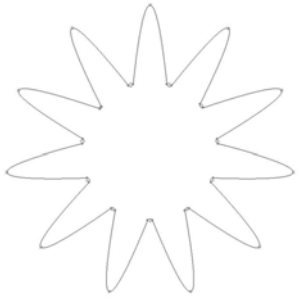

Figure 1: Demonstration non-standard acquisition trajectory

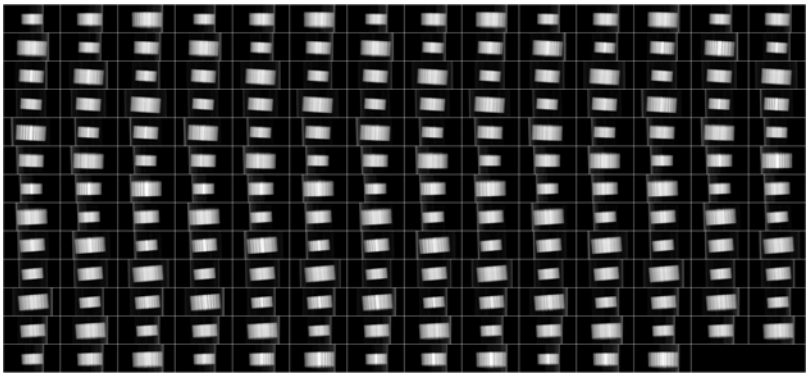

Figure 2: The resulting multi-magnification projection data acquired from the trajectory in Figure 1.

Figure 3: Left - Successful reconstruction from the data shown in Figure 2. Right - picture of phantom used in this study.

2) Advancements in dose-reduction techniques

Our ability to shape the field of view (region of radiation exposure) and adjust the magnification allows for high-resolution, region-of-interest interest at reduced radiation dose. This has allowed us to make advancements in reducing the radiation dose for clinically relevant imaging procedures.

For example, when a tumor is under treatment, its location is known, and we wish only to see the tumor and how it is responding to treatment. Tracking tumor response to treatment requires multiple scans, so reducing the dose for each scan is very desirable. We have accomplished a dramatic reduction in dose for this type of scan by the procedure described below.

First, we take a quick, sparse-projection preliminary scan – in this case, merely 20 projections. An example projection is shown to the right. Notice this data is untruncated. Below is a dimensioned drawing (in mm) and photo of the phantom being imaged.

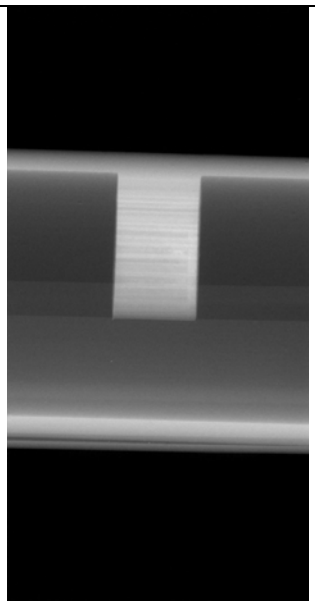

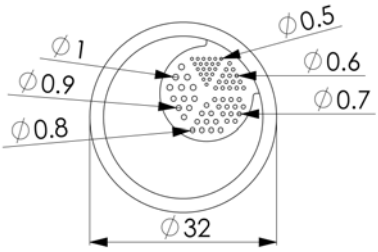

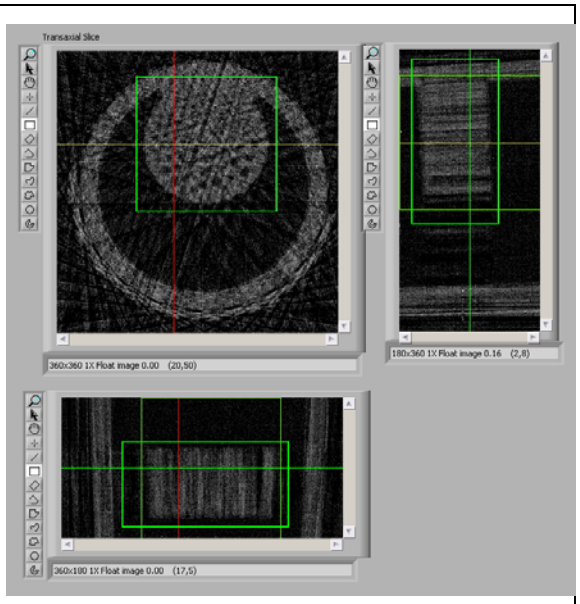

Next, the data from the scout scan are reconstructed and presented to a human observer. Although the reconstruction from sparse data is of low quality, it is enough to identify important anatomical markers. The human observer identifies a region of interest in the reconstruction with a computer mouse (shown as green box). The identified region of interest is used to guide the diagnostic scan

The CT system now adjust its magnification to fit the object, and the diagnostic scan is taken, limiting the field of of view to only the region of interest identified earlier. Example projections are shown below. Notice that x-ray radiation is not applied to the areas that are black.

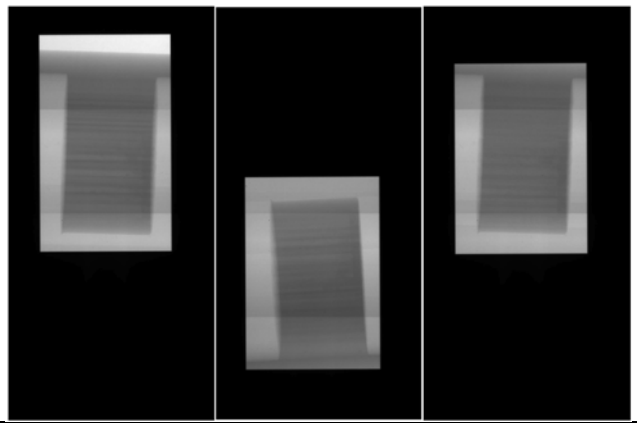

After the diagnostic scan is performed, we use the data gathered in the untruncated preliminary scan to predict the missing data from the diagnostic scan, thus overcoming the problem of reconstructing from truncated data. The result is a reconstruction clearly showing the region of interest and overall reduced radiation dose to the subject!

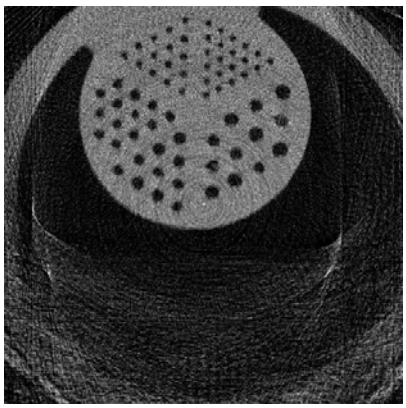

II.B.3. Global Compartmental Model

Compartmental models are widely used in pharmacokinetic studies in order to quantify the dynamics of the uptake and washout of tracer in organs, tumors and other tissues within the body. Conventional applications of compartmental models to imaging studies use an ad hoc approach where a separate compartmental model is used for each organ of interest, or even each voxel within an organ or tumor. These models could be called

local compartmental models and suffer from the drawback that they ignore the spatial movement of tracer. The common assumption is that this spatial movement is negligible compared to the movement of tracer between compartments within an organ, tumor or voxel. This assumption may be questionable, especially for high resolution systems where the voxels are very small.

The global compartmental model (GCM), as described in [1], is a method for rigorously combining traditional linear compartmental model with imaging. For the GCM we make the minimum number of assumptions needed to integrate a compartmental model with imaging. The first assumption is that the compartmental activities have a distribution in space as well as a time dependence. If the compartmental activities indeed represent something real, in the biological sense, then they would necessarily be distributed in space. The second assumption is that the observed spatio-temporal activity distribution in the PET or SPECT imaging system is a sum of these compartmental activity distributions. The third assumption is that integration of the compartmental activity distributions over their spatial supports gives the compartmental time-activity curves for the compartmental model. These spatial support regions may be arbitrarily selected regions, such as voxels, or anatomically based regions, such as organs or lesions. In the latter case the spatial support regions would be obtained via an anatomical imaging modality, such as CT or MRI. The fourth and final assumption is that the time-activity curves satisfy a linear compartmental model, i.e. a first order linear differential equation. These are the simplest kinetic models to analyze and are used extensively in pharmacokinetics. More complicated equations for the time-activity curves could be used also.

Associated with a linear compartmental model is a matrix of kinetic parameters that, along with an input function, govern the behavior of the time-activity curves. In [1] we showed that, in the absence of support information, we cannot identify all of these parameters from the SPECT or PET image alone. However, as the specificity of the support information increases, the number of identifiable parameters also increases. We found that the number of identifiable parameters can be computed from a symmetry group defined by the support information and number of compartments. Furthermore, this symmetry group can be used to precisely define the space of unidentifiable parameters, and thus map out our uncertainty in the kinetic parameter space.

Recently we have been studying the relation between the GCM and local compartmental models. For example, the most popular local model, with one compartment for each voxel, corresponds to what is called a mammillary model in the GCM. The standard method for analyzing this type of model is to measure activity in the vasculature by imaging a voxel in a large artery or in the heart. This time-activity curve is then taken as the input to the voxels in the region of interest, in the tumor, for example, in order to estimate the kinetic parameters for each voxel. This method has two drawbacks. The first is that the assumption that the input to the voxel from the vasculature is the measured blood-pool time-activity curve may not be valid. The second is that we do not end up with an estimate of all of the kinetic parameters in the GCM. On the other hand, by using the theory developed in [1] we can show that, in fact, all of the kinetic parameters in the mammillary GCM are identifiable without making any assumptions about the vascular input at each voxel. Thus the separate blood-pool measurement should be unnecessary. At present we are working on how to use this knowledge to develop a new method for estimating all of the kinetic parameters in the GCM for this type of system.

[1] Global Compartmental Pharmacokinetic Models for Spatiotemporal SPECT and PET Imaging E. Clarkson and M. A. Kupinski, *SIAM Journal on Imaging Sciences,* 2, 203-225, 2009

II.B.4. Evaluation of atherosclerotic development in Apo-E-deficient mice using FastSPECT II and ^{99m}Tc-labeled dual-domain cytokine ligand

Intense inflammatory response has been implicated as a critical factor in atherosclerosis destabilization and plaque rupture. We used ^{99m}Tc-TNFR2-Fc-IL-1ra, a dual-domain cytokine radioligand that can target inflammatory sites via interleukin-1β (IL-1β) and tumor necrosis factor-α (TNF-α) pathways, to investigate the development of atherosclerotic plaque in Apo-E-deficient (Apo-E-/-) mice that were fed an atherogenic diet. ^{99m}Tc-TNFR2-Fc-IL-1ra images with FastSPECT II were collected at age 20, 30, and 40 weeks in 8 Apo-E-/- mice and 6 Apo-E wild-type mice. After 3 mCi radiotracer injection, SPECT images were acquired at 1, 3, and 24 hours. At the end of the study session, the aortas and carotid arteries were harvested for autoradiograph imaging, histologic analysis, and immunohistochemical characterization.

Focal radioactive accumulations in the aorta region were found in the Apo-E-/- mice starting at age 20 weeks, but not in the control animals. As shown in Fig 1, radioactivity in the aortic focal u ptake was increased during the longitudinal study, suggesting growth and possibly destabilization of plaque. Around 30 weeks, the carotid arteries demonstrated focal radioactive uptake. Good consistency was found between radioactive uptake and atherosclerotic lesions, as well as a significant correlation between the radioactivity and inflammatory response as identified by ex vivo imaging and postmortem analysis.

Molecular imaging of atherosclerotic plaques using the dual-domain radioligand targeting TNF and IL-1 may provide a promising approach for understanding plaque development and inflammatory response.

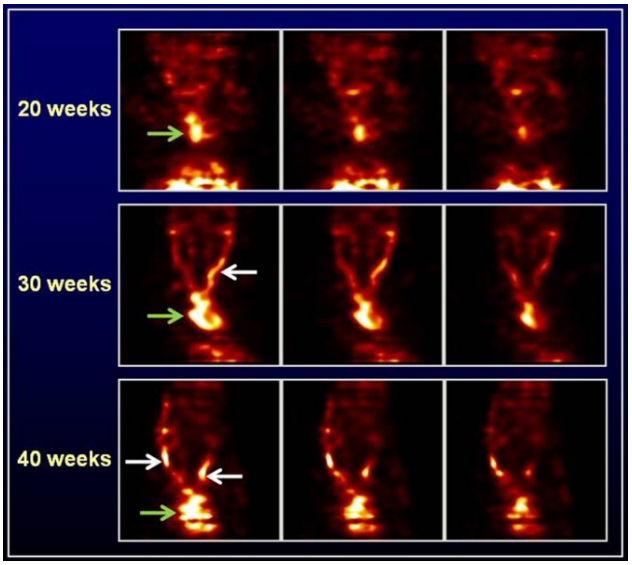

^{99m}Tc-TNFR2-Fc-IL-1ra SPECT images (selected coronal slices) in an Apo-E-/- mouse at age 20, 30, and 40 weeks. Focal radioactive accumulations were found in the aorta region (green arrows). The common carotid arteries demonstrated focal radioactive uptake (white arrows) starting at 30 weeks.

II.B.5. SPECT imaging of δ-opioid receptors using ^{111}In-labeled deltorphin-II ligand

δ-opioid receptors (DOR) are highly expressed in a variety of human tumors. We are collaborating with the Department of Chemistry of the University of Arizona to investigate an ^{111}In-labeled deltorphin-II ligand for *in vivo* imaging of DOR. We have preliminarily characterized *in vivo* kinetic profile and feasibility of this radioligand for tumor targeting in xenografted human HCT116 colon cancer.

The deltorphin-II ligand was generated by solid-phase peptide synthesis and linked with DOTA chelator for ^{111}In labeling. Specific competitive cell binding studies were performed in HCT116 human cancer cells expressing DOR. Xenografted tumors were grown for 10-18 days after subcutaneous implantation of 1 x 10^6 HCT116 cells in the right shoulder of nude mice. FastSPECT II imaging was performed in 6 mice expressing DOR (DOR+) and 5 wild-type control mice (DOR-). Immediately after i.v. injection of 7.4 MBq of radiotracer, dynamic images were acquired for 1 hr using a stationary small-animal SPECT imager. The animals were imaged again at 3 and 24 hrs post-injection. Tissue samples were harvested at the end of the imaging session for postmortem analysis.

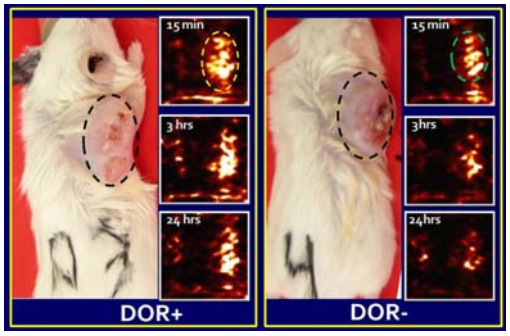

SPECT images of ^{111}In-labeled deltorphin-II ligand (selected coronal slices) in representative HCT116 xenograft with DOR+ (left panel) and DOR- (right panel). The radioactive accumulations in the tumors are marked with yellow and green dash.

In vitro competitive binding assays revealed that the ^{111}In-labeled ligand bound to cells expressing DOR with an IC_{50} value of 18 nM. DOR+ tumors were detectable at 15-30 minutes post-injection by FastSPECT II imaging and became well visualized at 3 hrs and increasingly prominent at 24 hrs. The DOR- tumors were initially visualized, but became less visible at 3 hrs and faintly visible at 24 hrs. The tumor/non-tumor ratios determined by ROI analysis were 1.62±0.21 for DOR- and 7.91±0.19 for DOR+ ($P < 0.01$) at 24 hrs.

Our imaging results indicate that the deltorphin-II radioligand may provide a new approach to study the expression of δ-opioid receptors in tumor growth and metastasis.